Astronomy
&
Astrophysics

The fate of S-bearing species after ion irradiation of interstellar icy grain mantles

M. Garozzo[1], D. Fulvio[1,2], Z. Kanuchova[1,3], M. E. Palumbo[1], and G. Strazzulla[1]

[1] INAF - Osservatorio Astrofisico di Catania, via S. Sofia 78, 95123 Catania, Italy
e-mail: [mga;mepalumbo]@oact.inaf.it
[2] Dipartimento di Fisica e Astronomia, Università di Catania, Italy
[3] Astronomical Institute of Slovak Academy of Science, 059 60, T. Lomnica, Slovakia

ABSTRACT

Context. Chemical models predict the presence of S-bearing molecules such as hydrogen sulfide (H_2S) in interstellar icy grain mantles in dense molecular clouds. Up to now only two S-bearing molecules, namely sulfur dioxide (SO_2) and carbonyl sulfide (OCS), have been detected in the solid phase towards young stellar objects (YSOs), while upper limits for solid H_2S have been reported towards the same lines of sight. The estimated abundance of S-bearing molecules in icy grain mantles is not able to account for the cosmic S abundance.
Aims. In this paper we studied the effects of ion irradiation on different icy targets formed by carbon monoxide (CO) and SO_2 or H_2S as mixtures and, for the first time, as layers.
Methods. We carried out several irradiation experiments on ices containing SO_2 or H_2S mixed or layered with CO. The samples were irradiated with 200 keV protons in a high-vacuum chamber ($P < 10^{-7}$ mbar) at a temperature of 16–20 K. IR spectra of the samples were recorded after various steps of irradiation and after warm-up.
Results. We have found that the column density of H_2S and SO_2, as well as CO, decreases after irradiation, and the formation of new molecular species is observed. In the case of $CO:SO_2$ samples, OCS, sulfur trioxide (SO_3), ozone (O_3), and carbon dioxide (CO_2) are the most abundant species formed. In the case of $CO:H_2S$ samples the most abundant species formed are OCS, SO_2, carbon disulfide (CS_2), hydrogen persulfide (H_2S_2), and CO_2. The profile of the OCS band formed after irradiation of the $CO:H_2S$ mixture compares well with the profile of the OCS band detected towards the high mass YSO W33A.
Conclusions. Our results show that on a time scale comparable to the molecular cloud lifetime, the column density of H_2S is strongly reduced and we suggest that this could explain the failure of its detection in the solid phase in the lines of sight of YSOs. We suggest that the solid OCS and SO_2 detected in dense molecular clouds are formed after ion irradiation of icy grain mantles.

Key words. astrochemistry – molecular processes – methods: laboratory – techniques: spectroscopic, ISM: molecules – ISM: abundances

1. Introduction

Observations of various astrophysical environments show that ices are very common in the Universe. They can be found in the Solar System (on the surface of planets, satellites, comets and other minor objects), as well as in the interstellar medium, inside dense molecular clouds where, due to the low temperature ($\sim$10 K) and high density ($\geq$10^4 H cm^{-3}), gas species freeze out on dust grains forming icy mantles. When the ices are exposed to particle fluxes (cosmic ions, solar wind, etc.), they are modified chemically and structurally. Incoming ions release their energy into the target and destroy molecular bonds producing fragments that, by recombination, form new molecules, also different from the original ones and, in general, also with a new lattice structure. This explains the change of spectral behavior of irradiated surfaces (Brunetto et al. 2006) as well as the chemical composition of cometary (e.g. Strazzulla et al. 1991) or interstellar (e.g. Palumbo et al. 2000) ices. Thus, the laboratory simulations of ion irradiation on different materials (ices) is key in understanding their evolution within the Solar System and in the interstellar medium. In this paper, we have focused on the study of the alterations induced by cosmic ion bombardment of S-bearing molecules in the icy mantles of dust grains in dense molecular clouds. Until now, only two S-bearing molecules – sulfur dioxide (SO_2) and carbonyl sulfide (OCS) – have been detected in icy grain mantles (e.g. Boogert et al. 1996, 1997; Zasowski et al. 2009; Palumbo et al. 1995, 1997), while the presence of hydrogen sulfide (H_2S) has been suggested (e.g. Geballe et al. 1985) although it has never been firmly identified, probably because its main band near 3.92 μm overlaps with a feature of methanol (CH_3OH). The gaseous OCS molecules observed in hot cores are thought to have originated on dust grains (Hatchell et al. 1998). The parent molecules of OCS are not yet known. Ferrante et al. (2008) recently suggested that OCS is a product of ion irradiation of a mixture of CO and H_2S ice. For our study, we carried out several irradiation experiments on ices containing SO_2 and H_2S pure or mixed with carbon monoxide (CO). Although models of interstellar ices propose that their compounds are mixed together, recent observations suggest that interstellar ices are best represented by a layered ice model rather than mixed ice (Fraser et al. 2004; Palumbo 2006). For this reason, we have performed experiments with different kinds of icy targets. Some targets were prepared by a co-deposition of a mixture of two gas compounds at low temperature (CO and SO_2 or H_2S) and others by a deposition of an SO_2 or H_2S layer subsequently covered with a CO layer. The substrate for the experiments was a

Table 1. Details of experiments performed and discussed in this work.

Sample	Substrate	T(K)	Ion	E(keV)
CO:SO_2 = 5:1 mixture	Si	16	H$^+$	200
CO/SO_2 layer	Si	16	H$^+$	200
CO:H_2S = 10:1 mixture	Si	20	H$^+$	200
CO:H_2S = 1:10 mixture	KBr	20	H$^+$	200
CO/H_2S layer	KBr	20	H$^+$	200

silicon wafer or a KBr pellet. To our knowledge, the layered ones are the first experiments ever performed to study the chemistry induced at the interface between two icy species, while irradiation experiments with different gases and gas mixtures deposited on a refractory substrate at low temperature are more common (Mennella et al. 2004; Gomis & Strazzulla 2005, 2008; Moore et al. 2007a; Loeffler et al. 2006). Details of all the experiments performed and discussed in this work are listed in Table 1. The thickness of all the targets was smaller than the penetration depth of the used ions (200 keV H$^+$); so, after the energy release into the material, the passing ions were implanted in the (silicon or KBr) substrate on which ices had been deposited.

2. Experimental apparatus

The experiments were performed in a high-vacuum chamber ($P < 10^{-7}$ mbar) facing, through KBr windows, a FTIR spectrophotometer (Bruker Vertex 70) working in the spectral range 8000–400 cm^{-1} (1.25–25 μm) with a resolution of 1 cm^{-1}. Preprepared gases (or mixtures) are admitted into the chamber by a needle valve and accreted in the form of ices on a silicon or KBr substrate placed in thermal contact with the tail section of a closed-cycle helium cryostat, whose temperature can vary from 10 to 300 K. During the deposition, the thickness of the growing ice film is monitored by a He-Ne laser interference fringe system (Baratta & Palumbo 1998; Fulvio et al. 2009). Ions are obtained from a 200 kV ion implanter (Danfysik 1080–200) which is interfaced to the vacuum chamber. The ion beam current densities are maintained below 1 μA cm^{-2} to avoid macroscopic heating of the target. The substrate plane forms an angle of 45° with the IR beam of the spectrometer and the ion beam (the two being mutually perpendicular) so transmittance spectra can be easily obtained in situ, without tilting the sample. Each time, two IR spectra were recorded, selecting the electric vector parallel (P polarization) and perpendicular (S polarization) to the plane of incidence. The polarization is selected using a rotatable polarizer placed in the path of the infrared beam in front of the detector. It has been shown (Baratta et al. 2000; Palumbo et al. 2006) that when the band profiles recorded in P and S polarization are similar, the transitions are weak and the features seen in the transmission spectra directly reflect the variation of the absorption coefficient of the solid sample. This circumstance was observed for the profile of all the new bands present in the spectra after ion irradiation. For the study of these bands, P spectra were considered since the signal to noise ratio is higher for this polarization. On the other hand, the profile of the CO and SO_2 bands in the layered samples are different in P and S spectra. In P spectra LO-TO splitting is observed (Baratta & Palumbo 1998; Palumbo et al. 2006). All spectra shown in the following have been taken in P polarization.

After irradiation, targets were warmed at a rate of a few degrees/minute up to sublimation of the sample and some spectra were taken at chosen temperatures in the range 20–150 K. For more details on the experimental setup the reader is

Table 2. Thickness and density of the samples, stopping powers and the investigated dose ranges.

Sample	Thickness (μm)	ϱ (g cm^{-3})	Stopping^a (eV Å^{-1})	Dose range (eV/16 u)
CO:SO_2 = 5:1	0.776	0.99^b	7.5	1.3–80.7
CO/SO_2 layer	0.480/0.318	0.8^c/1.93^d	6.2/14.2	1.3–39.8
CO:H_2S = 10:1	0.662	0.83^b	6.6	1.3–42.2
CO:H_2S = 1:10	0.356	1.26^b	10.0	1.3–42.1
CO/H_2S layer	0.325/0.148	0.8^c/1.31^b	6.1/10.8	1.3–42.2

Notes. $^{(a)}$ Stopping power of 200 keV protons calculated by the SRIM software (Ziegler et al. 1996) ; $^{(b)}$ this work ; $^{(c)}$ Loeffler et al. (2005) ; $^{(d)}$ Rudolph (1977) .

Table 3. List of integrated band strength (A) values used.

Molecule	Band (cm^{-1})	A (cm molecule^{-1})	Reference
H_2S	2550	2.9×10^{-17}	Smith (1991)
CO_2	2345	7.6×10^{-17}	Yamada & Person (1964)
CO	2139	1.1×10^{-17}	Jiang et al. (1975)
^{13}CO	2092	1.1×10^{-17}	Jiang et al. (1975)
OCS	2050	1.5×10^{-16}	Hudgins et al. (1993)
CS_2	1520	9.13×10^{-17}	Pugh & Rao (1976)
SO_2	1341	1.47×10^{-17}	Garozzo et al. (2008)
O_3	1040	1.4×10^{-17}	Smith et al. (1985)

referred to Strazzulla et al. (2001). By measuring the ion fluence (ions cm^{-2}), which is related to the ion current measured during the irradiation, and using the SRIM software (Ziegler et al. 1996) to calculate stopping powers, we can determinate, for each experiment, the radiation doses of the target, on a scale of eV per 16 u molecule, where u is the unified atomic mass unit. In Table 2 details of the samples that have been used in our experiments are given. The thickness and density values have been obtained following the same procedure described in Fulvio et al. (2009).

The column density N (molecules cm^{-2}) of a given species was calculated using the following equation:

$$N = \frac{\int \tau_\nu \mathrm{d}\nu}{A} \tag{1}$$

where $\int \tau_\nu \mathrm{d}\nu$ (cm^{-1}) is the integrated area (on an optical depth scale) calculated after subtraction of the underlying continuum and A is the integrated band strength (cm molecule^{-1}). The A-values used are listed in Table 3.

In some cases, the normalized column density of molecules was calculated, i.e. the ratio N/N_i, where N_i is the initial column density of the parent molecule and N is the column density of the molecule at some point of the irradiation experiment.

3. Results

Before discussing the results obtained in this work, we summarize previous results concerning the irradiation of pure CO, SO_2 and H_2S ices. The results of H$^+$ irradiation of pure CO ice at low temperature (10–80 K) have been discussed by Palumbo et al. (2008). The formation of abundant carbon dioxide (CO_2) and several carbon chain oxides such as dicarbon monoxide (C_2O), tricarbon monoxide (C_3O) and tricarbon dioxide (C_3O_2) is described therein. Effects of the irradiation of pure SO_2 ice with protons of different energies at different temperatures (from 16
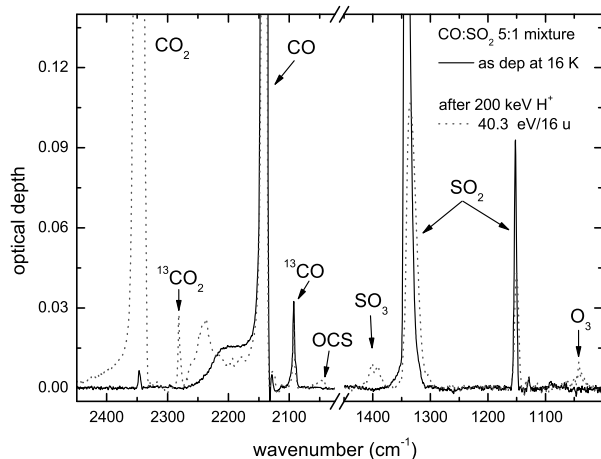
Fig. 1. IR transmittance spectra of $CO:SO_2 = 5:1$ mixture as deposited at 16 K and after 200 keV H^+ irradiation.

Table 4. Peak position of IR bands of unirradiated $CO:SO_2$ ice as a mixture and layered sample.

Wavenumber (cm^{-1})		Molecule
mixture	layered	
2139	2139	CO
2092	2092	^{13}CO
1341	1344	SO_2
1152	1152	SO_2

to 88 K) have been well studied and the formation of the sulphur trioxide (SO_3), SO_3 in a polymeric form (Moore 1984; Garozzo et al. 2008) and ozone (O_3; Garozzo et al. 2008) was observed. Results of the irradiation of pure H_2S ice at low temperature (50 and 16 K) can be found in Moore et al. (2007b) and in Strazzulla et al. (2009). They agree that the only molecule detected after irradiation is hydrogen persulfide (H_2S_2).

3.1. Irradiation of $CO:SO_2 = 5:1$ mixture

In Fig. 1 we plot the IR transmittance spectra of a thin film of $CO:SO_2 = 5:1$ ice mixture as deposited at 16 K and after irradiation with 200 keV H^+.

In the spectrum of deposited ice, the main features at 1341 and 1152 cm^{-1} are attributed to the ν_3 asymmetric and ν_1 symmetric stretching modes of the SO_2 molecules, while the band at 2139 cm^{-1} is attributed to the ν_1 stretching mode of the CO molecules (Table 4).

After proton irradiation, new bands appear in the spectrum, which indicate the formation of other molecules: not only abundant CO_2 (2347 cm^{-1}), but also SO_3 (see the doublet centred at about 1400 cm^{-1}), O_3 (1041 cm^{-1}), C_3O_2 (2193, 2241 cm^{-1}) and OCS (2050 cm^{-1}). A list of peak positions and the assignment of the newly formed bands is given in the Table 5.

In Fig. 2 we report the SO_2 (bottom panel) and CO (top panel) normalized column density as a function of the irradiation dose. The SO_2 column density has been calculated using the ν_3 band area (cm^{-1}) centred at 1341 cm^{-1}, while the CO column density has been calculated using the band area centred at 2092 cm^{-1} due to ^{13}CO – the band of ^{12}CO at 2139 cm^{-1} being saturated. It is clear that the SO_2 and CO column densities decrease as the dose increases, due to the fact that part of the SO_2 and CO molecules are transformed into new species. However, the SO_2 column density has a sharp drop-off followed by a much

Table 5. Peak position of the bands formed after irradiation of $CO:SO_2$ as mixture and layered sample.

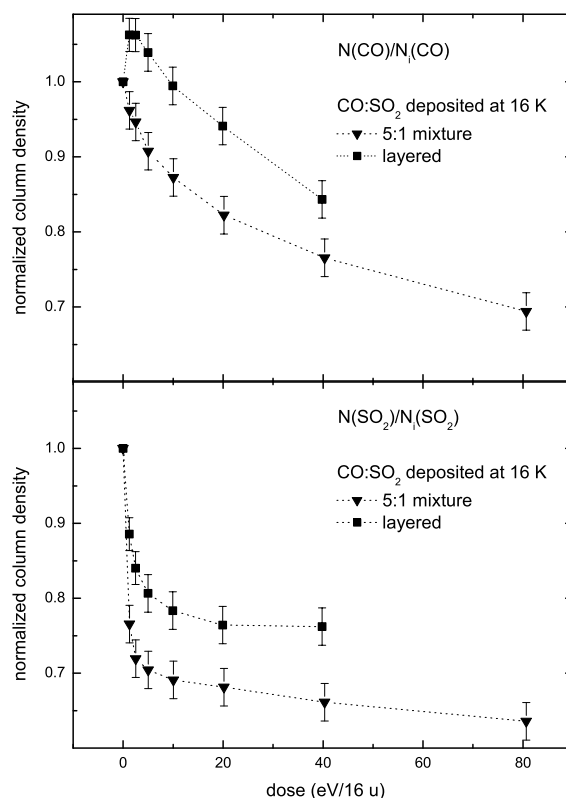| Wavenumber (cm^{-1})		Molecule
mixture	layered	
3708	3708	CO_2
	2399	C_3O_2
2347	2346	CO_2
2281	2281	$^{13}CO_2$
	2248	C_3O
2241	2242	C_3O_2
	2212	C_5O_2
2193	2193	$OCC^{13}CO$
	2180	C_7O_2
	2123	C_7O_2
	2062	C_5O_2
2050	2050	OCS
	1989	C_2O
1875	1875	
1392–1401	1390–1402	SO_3
	1205–1229	poly SO_3
	1075	SO_3
1041	1038	O_3
659	660	CO_2

Fig. 2. Normalized column density of CO and SO_2 as a function of dose in $CO:SO_2 = 5:1$ mixture ice at 16 K and in CO deposited on SO_2 at 16 K. Points are connected for clarity.

less rapid decline. The CO destruction follows a more uniform behavior.

Figure 3 shows the column density of CO_2, inferred from the band centred at 2347 cm^{-1}, of O_3 inferred from the band at 1041 cm^{-1} and of OCS (from the band at 2050 cm^{-1}). To calculate these column densities we used the integrated band strength values given in Table 3. For the SO_3 doublet centred at about
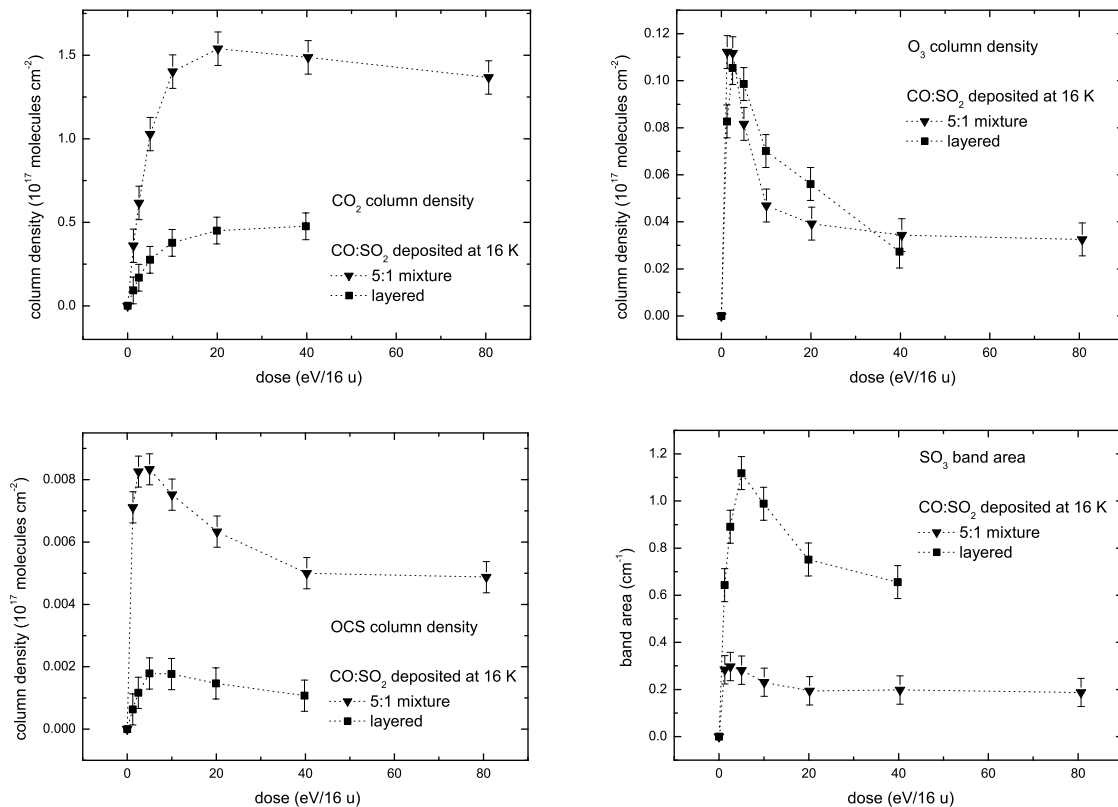
Fig. 3. The column densities of CO_2, O_3, and OCS and the band area of the SO_3 doublet after 200 keV proton irradiation of $CO:SO_2$ mixture or layered ices at 16 K as a function of dose. Data points are connected for clarity.

1400 cm^{-1} we report the band area, because, as far as we know, the integrated band strength has not been measured.

SO_3, O_3 and OCS show the same trend. They increase very fast at low doses, at doses higher than 6 eV/16u the column densities decrease rapidly until equilibrium between destroyed and newly formed molecules is reached. This behavior is consistent with that of the parent molecule SO_2 which, as said, is rapidly destroyed. The CO_2 column density increases slowly and slowly decreases when the dose is higher than 20 eV/16u.

3.2. Irradiation of CO ice deposited on top of a SO_2 layer

We performed a second kind of experiment. A layer of pure SO_2 was deposited onto a silicon substrate at 16 K and then a layer of pure CO was deposited onto the previous layer. This target was irradiated with 200 keV protons. In Fig. 4 we plot the IR transmittance spectra of the $CO:SO_2$ layered ice as deposited at 16 K and after irradiation with 200 keV H$^+$.

The main features in the spectrum of deposited ice appear at 1344, 1152 and 2139 cm^{-1}. They are attributed to the ν_3 and ν_1 stretching modes of the SO_2 molecules and ν_1 stretching mode of the CO molecules, respectively (Table 4). We notice that the profile of the CO band shows two peaks at 2142 cm^{-1} and 2139 cm^{-1} due to the LO and TO mode respectively (Palumbo et al. 2006). Peak positions of the newly formed bands and their assignment are listed in Table 5. The new molecules which have been formed after ion irradiation are the same as those obtained in the irradiation experiment with, separately, pure SO_2 (Garozzo et al. 2008) and pure CO (Palumbo et al. 2008). In addition, OCS (2050 cm^{-1}) is produced at the interface between the two layers. Also in this case we calculated the SO_2, CO normalized column densities, CO_2, O_3, OCS column densities

(molecules cm^{-2}) and measured the SO_3 band area (cm^{-1}) at different doses (Figs. 2 and 3). These column densities show the same trend as they have in the case of the mixture, except for CO that seems to increase at low doses. This is not a real growth but an effect due to the variation of the integrated absorbance of CO during irradiation. This effect was described by Loeffler et al. (2005) and it is also known for the 3 μm band of water ice and has been studied by Leto & Baratta (2003).

3.3. Irradiation of $CO:H_2S$ mixtures

Additional experiments were performed to study the irradiation of CO and H_2S ice mixtures. We have prepared two mixtures with different ratios of CO to H_2S: 10:1 (mixture 1) and 1:10 (mixture 2). IR transmittance spectra of mixtures 1 and 2 deposited at 20 K and after irradiation with 200 keV H$^+$ are plotted in Fig. 5.

Mixture 1: In the spectra of deposited ice there are four main features: those at 2608 and 2571 cm^{-1} are due to the ν_3 and ν_1 stretching modes of the H_2S molecules, those at 2139 and 2092 cm^{-1} are due to ν_1 stretching modes of the CO and ^{13}CO molecules respectively (Table 6). The band of CO at 2139 cm^{-1} is saturated, thus to have information on the trend of CO during the irradiation we have used the band of ^{13}CO.

The new molecules formed after ion irradiation of the mixture 1 (rich in CO) are listed in Table 7. Two new species, OCS (2043 cm^{-1}) and carbon disulfide CS_2 (1519 cm^{-1}), containing both C and S atoms were identified. Other S-bearing molecules detected after irradiation are H_2S_2 (2486 cm^{-1}) and SO_2 (1327 cm^{-1}, 1149 cm^{-1}).
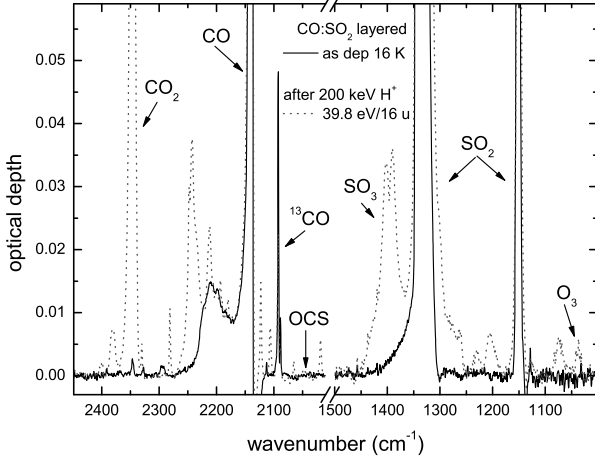
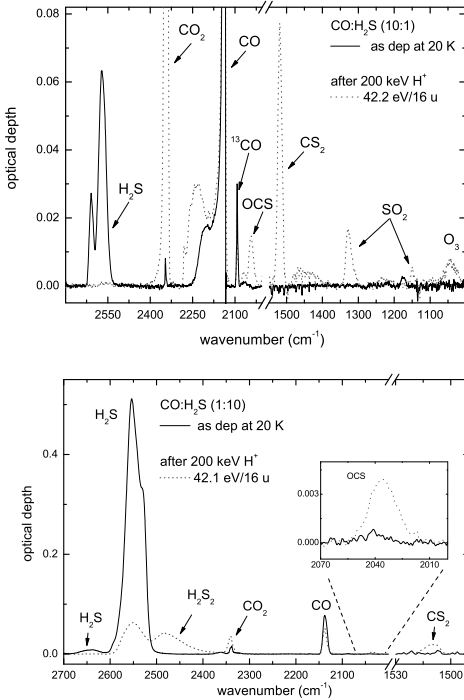**Fig. 4.** IR transmittance spectra of the CO:SO$_2$ layered ice as deposited at 16 K and after irradiation with 200 keV H$^+$.

Table 6. Peak position of the IR bands of unirradiated CO:H$_2$S ice a 10:1 mixture (mixture 1) and a 1:10 mixture (mixture 2) and of a layered film.

Wavenumber (cm^{-1})			Molecule
mixture 1	mixture 2	layered	
2608	2640	2642	H$_2$S
2571	2553	2546	H$_2$S
2139	2138	2139	CO
2092	2090	2092	^{13}CO

Table 7. Peak position of bands formed after irradiation of CO:H$_2$S ice mixtures 10:1 (mixture 1) and 1:10 (mixture 2) and of a layered film.

Wavenumber (cm^{-1})			Molecule
mixture 1	mixture 2	layered	
3707		3707	CO$_2$
2486	2489	2487	H$_2$S$_2$
		2399	C$_3$O$_2$
2345	2338	2346	CO$_2$
2281		2280	^{13}CO$_2$
2258			
2247		2248	C$_3$O
2243		2242	C$_3$O$_2$
2229			
2214		2212	C$_5$O$_2$
2192		2192	OCC^{13}CO
2122		2122	C$_7$O$_2$
2070		2061	C$_5$O$_2$
2043	2037	2040	OCS
1989		1989	C$_2$O
1858		1858	HCO
1519	1515		CS$_2$
1327			SO$_2$
1149			SO$_2$
1044			O$_3$
658		659	CO$_2$

Fig. 5. IR transmittance spectra of CO:H$_2$S 10:1 (mixture 1 – *top panel*) and 1:10 (mixture 2 – *bottom panel*) as deposited at 20 K and after irradiation with 200 keV H$^+$.

The normalized column densities of H$_2$S and CO using the band area centred at 2571 cm^{-1} and 2092 cm^{-1} of ^{13}CO respectively are shown in Fig. 6.

Both CO and H$_2$S column densities decrease as dose increases due to the fact that these molecules are sputtered away or transformed into a new species. An extrapolated value for the sputtering yield of a surface of CO exposed to vacuum for 200 keV protons is 10 CO/proton (Brown et al. 1984), which means that about 3% of the material would have been removed at the highest fluence.

In Fig. 6 we show the normalized column density of CO$_2$ (from the band peaked at 2345 cm^{-1}), CS$_2$ (1519 cm^{-1}), OCS (2043 cm^{-1}), SO$_2$ (1327 cm^{-1}) and the band area of H$_2$S$_2$ at 2486 cm^{-1} (the integrated band strength of H$_2$S$_2$ is not known) as a function of dose.

At low doses, in agreement with the rapid destruction of the H$_2$S molecules, we observe the formation of new S-bearing molecules H$_2$S$_2$, CS$_2$, SO$_2$ and OCS. At a dose of about 5 eV/16u there are not enough H$_2$S molecules to form new H$_2$S$_2$, and, moreover, existing H$_2$S$_2$ molecules are decomposed until its column density decreases to zero. OCS molecules are also slowly decomposed. The sulfur atoms, originating in H$_2$S, are used to build up mainly SO$_2$ and CS$_2$ molecules. However, at the end of the experiment, the total amount of detected sulfur atoms, in the form of CS$_2$, SO$_2$ and OCS, is roughly 4×10^{16} atoms cm^{-2}, while at the beginning, the amount of the sulfur in the target was about 7×10^{16} atoms cm^{-2} (the column density was considered). This means that a certain fraction of sulfur atoms has been sputtered and a fraction has formed a sulfur-rich residuum that is the source of sulfur atoms to build up SO$_2$, CS$_2$ and OCS after the total decomposition of H$_2$S (e.g. Strazzulla et al. 2009).

Mixture 2: In the spectrum of deposited ice (see Fig. 5), three main features appear: two (at 2640 and 2553 cm^{-1}) are due to the ν_3 and ν_1 stretching modes of the H$_2$S molecules, and one at 2138 cm^{-1} is due to the ν_1 stretching mode of the CO molecules (Table 6). The column densities of CO and H$_2$S are shown in
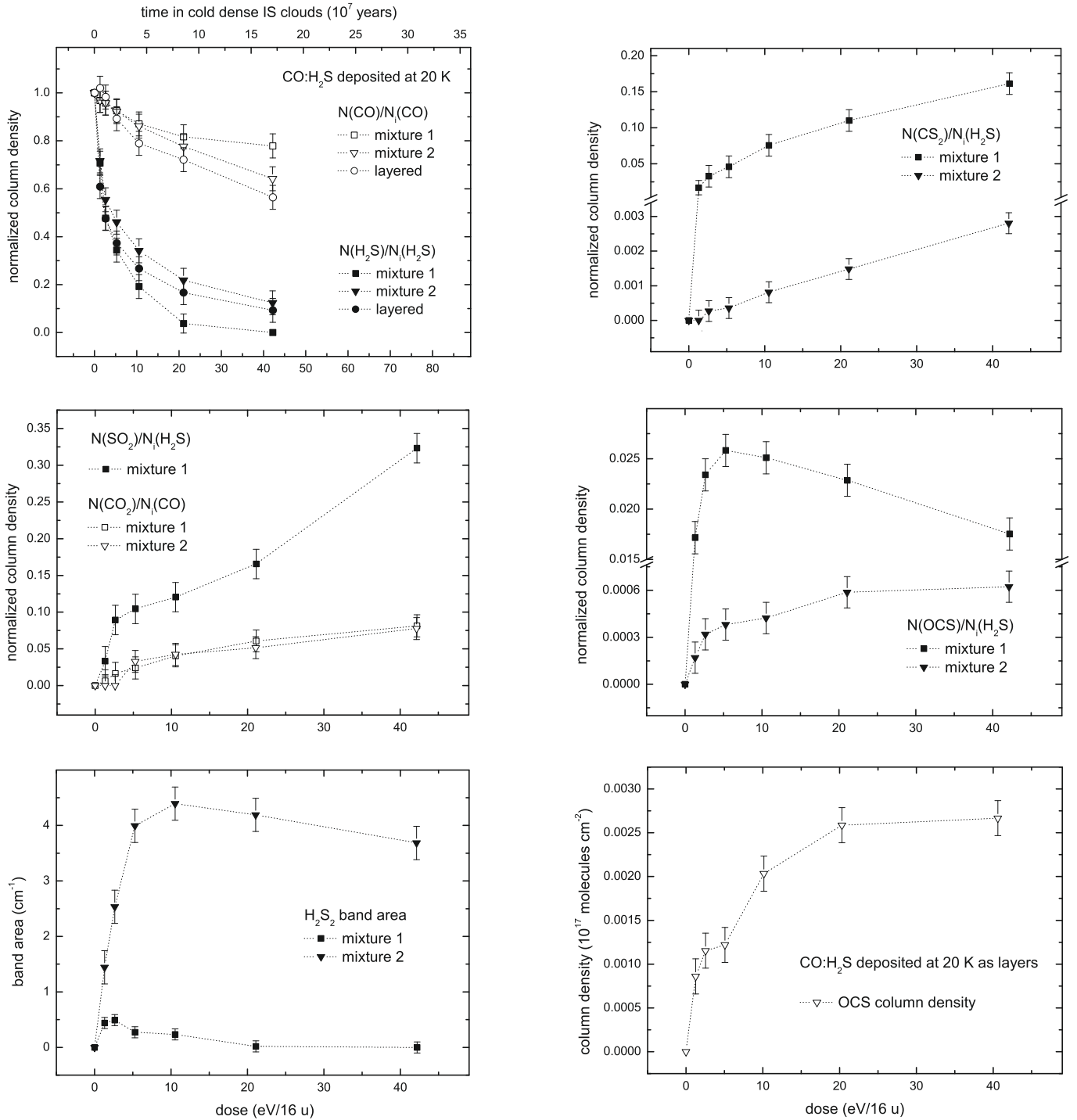
Fig. 6. Normalized column density of CO, H_2S, CO_2, CS_2, OCS, SO_2 and the band area of H_2S_2 at 2486 cm^{-1} in CO:H_2S mixtures 10:1 (mixture 1) and 1:10 (mixture 2) plotted as a function of dose. Column densities of CO, H_2S and OCS, in CO:H_2S layered as a function of dose are also shown. The equivalence between the doses used in laboratory and the time scale in cold dense IS clouds (1 eV/16u $\cong$ 4 million years) is calculated by assuming an effective flux of monoenergetic protons (1 MeV) of 1 H$^+$ cm^{-2} s^{-1} in the IS clouds (Mennella et al. 2003). For details on calculations see Appendix A. Data points are connected for clarity.

Fig. 6 as a function of dose. As expected, the two molecular species were decomposed during irradiation, CO is reduced to 80% of its initial value and H_2S, as in the case of mixture 1, is almost completely destroyed. Proton irradiation causes the formation of the same molecules as in the case of irradiation of mixture 1, except for the carbon chains oxides and SO_2. The normalized column densities of the molecules formed are plotted in Fig. 6 as a function of the dose. The trends of the column density of CS_2 and CO_2 are similar to those in the case of irradiation of

mixture 1. However, the rate of decomposition and rebuilding of H_2S_2 and OCS molecules is different with respect to the previous experiment because of the different relative amount of parent species in the two mixtures.

3.4. Irradiation of CO deposited on top of H_2S ice

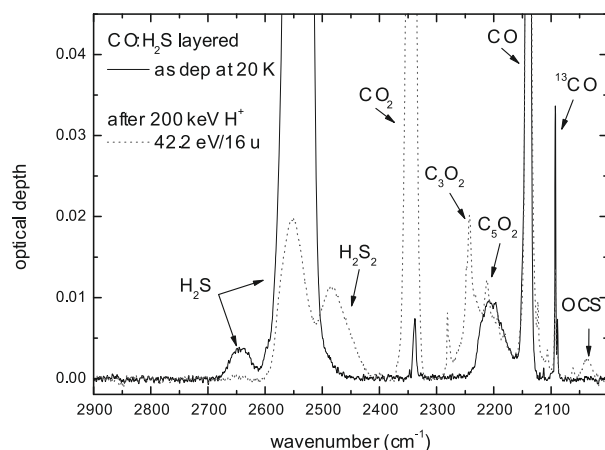An additional experiment was the irradiation of CO and H_2S ices in the form of layers. The target was prepared in the same

Fig. 7. IR transmittance spectra of the CO:H_2S layered ice as deposited at 20 K and after irradiation with 200 keV H$^+$.

way as the target in the experiment described in Sect. 3.2. The IR spectra of the sample before irradiation and as deposited at 20 K is plotted in Fig. 7. Except OCS, all the molecules formed by irradiation are the same as were formed by the irradiation of pure CO and pure H_2S ices. OCS molecules were formed at the interface of the two layers.

Because the column density for all the newly formed molecules follows a similar trend as in the case of pure CO and pure H_2S irradiation, just the OCS column density as a function of dose is presented in Fig. 6. The trend of OCS column density formed at the interface of two ices is similar to that found for the irradiated mixture rich in H_2S.

3.5. Warm-up effects

After the end of irradiation, all icy samples were warmed up to room temperature and spectra recorded at different temperatures. During warm-up the peak position of the OCS band shifts. This shift depends on the initial mixture. As an example, in the case of the CO:H_2S = 10:1 mixture the peak shifts from 2043 cm^{-1} at 20 K to 2038 cm^{-1} at 100 K. In this mixture the 1327 cm^{-1} SO_2 band also shifts to lower wavenumbers after warm-up.

4. Discussion and conclusions

In this paper, we have studied the effects of ion irradiation of different icy targets formed by CO and SO_2 or H_2S as mixtures and, for the first time, have separated layers. Our main results are:

1) The production of OCS is observed in all the experiments considered here using as targets CO:SO_2 or CO:H_2S deposited as mixtures or layered. Since the thickness of the interface of two layered ices (mixing of materials) is lower than the total thickness of deposited mixtures, the total amount of produced OCS is lower in the case of ion irradiation of the layered ices. Moreover, in the cases of irradiation of CO:H_2S samples, CS_2 was formed.
2) An important finding is that H_2S column density has a very rapid drop off at the beginning of irradiation, until almost all the H_2S molecules are decomposed.
3) The production of carbon chain oxides is observed only for the mixtures rich in CO and in the layered samples.
4) One of the products of ion irradiation of targets containing SO_2 is ozone (O_3). This result confirms and extends previous

findings discussed in Garozzo et al. (2008). A small amount of ozone is detected also in the CO:H_2S = 10:1 mixture. In this case, the formation of O_3 is due to the high abundance of CO_2 (Loeffler et al. 2005; Strazzulla et al. 2005) in the final stages of irradiation.
5) In the case of the CO:H_2S mixtures, only in the one rich in CO (i.e. also rich in oxygen) are the SO_2 molecules detected after irradiation. Similarly, Moore et al. (2007b) reported the formation of sulfur dioxide as a result of irradiation of ice mixtures rich in oxygen (H_2O:H_2S = 8:1). O_3 molecules also are detected only after irradiation of the CO:H_2S = 10:1 sample.
6) The amount of OCS produced by irradiation depends not only on the kind of sulfur-bearing species but also on the amount of CO involved in the process.

Ferrante et al. (2008) presented several experiments on the formation of OCS in proton irradiated ices at 10 K. Our results are generally in agreement with those of Ferrante et al. (2008). Particularly, OCS is produced more efficiently in a mixture CO:H_2S, in which CO is more abundant with respect to H_2S. As well as Ferrante et al. (2008), we have observed a shift of the OCS band peak position during heating and this shift depends on the kind of sample in which the OCS was formed. Furthermore, Ferrante et al. (2008) do not report – for their experiment on the CO:H_2S = 5:1 mixture – the detection of O_3 and SO_2 molecules. This can be due to the different mixture ratio used compared to our experiment (10:1).

So far, only two S-bearing molecules, SO_2 and OCS, have been detected in the icy mantles of the dust grains of the interstellar medium (e.g. Boogert et al. 1996, 1997; Zasowski et al. 2009; Palumbo et al. 1995, 1997). In Table 8 we report the abundances measured in some Young Stellar Object (YSO) sources. Geballe et al. (1985) reported the identification of solid H_2S after detection of a band at about 3.9 μm toward the high mass YSO W33A but further observations have shown that the 3.9 μm band is due to methanol (Grim et al. 1991; Allamandola et al. 1992). Upper limits of H_2S column density towards other lines of sight are given in Smith (1991). The role of H_2S as a precursor of OCS and, possibly, SO_2 in the icy mantles of dust grains in the interstellar medium is not well understood. H_2S in solid phase has never been identified in any YSOs, although models of envelopes of YSOs predict large quantities of H_2S on grain surfaces formed by hydrogenation of sulfur atoms (e.g. Garrod et al. 2007). The results of our experiments on targets containing H_2S show that this molecule, under the effect of ion irradiation, is reduced to 4% of its initial value after 21 eV/16u, which corresponds to about 8×10^7 years in the cold and dense interstellar clouds (see Fig. 6. For the calculation of the correspondence between the irradiation dose in laboratory and the time in the dense interstellar clouds, see Appendix A). This time closely compares with the evolution time of dense clouds which ranges from 3 to 50×10^7 years (Greenberg 1982). This could explain the failure of H_2S solid phase detection in the interstellar medium. According to our experimental results, after the same dose (21 eV/16u), the missing H_2S is converted into OCS (2.3%), CS_2 (12%), SO_2 (16%) and a refractory residue.

We have compared the profile of the laboratory band of OCS at different temperatures (in the interval 20 to 100 K) with the band of OCS observed toward W33A. No single spectrum fits the observed OCS band perfectly, but using two components, namely that at 20 K (representing unheated regions) and 60 K (representing the dust heated by the YSO), a good fit was obtained (see Fig. 8). The use of spectra at two different

Table 8. Abundances, relative to solid H_2O and total H, of the S-bearing species detected in the icy grain mantles.

Source	Abundances			
	$N(OCS)/N(H_2O)$	$N(SO_2)/N(H_2O)$	$N(OCS)/N(H)^a$	$N(SO_2)/N(H)^a$
Mon R2 IRS 2	5.5×10^{-4b}		3.2×10^{-8b}	
AFGL 989	1.0×10^{-3b}		2.3×10^{-8b}	
W33A	4.0×10^{-4b}	$(3.1 \pm 1.6) \times 10^{-3c}$	7.0×10^{-8b}	$(6.2 \pm 3.2) \times 10^{-7c}$
NGC 7538 IRS 1	$<5.0 \times 10^{-4d}$	$(8.0 \pm 2.0) \times 10^{-3c}$	$<7.6 \times 10^{-9d}$	$(1.2 \pm 0.3) \times 10^{-7c}$
NGC 7538 IRS 9	5.0×10^{-4e}	$<5.0 \times 10^{-3c}$	3.4×10^{-8e}	$<3.4 \times 10^{-7c}$

Notes. [a] N(H) column densities are taken from Tielens et al. ([1991]) and Boogert et al. ([1997]); [b] Palumbo et al. ([1997]); [c] Boogert et al. ([1997]); [d] Gibb et al. ([2004]); [e] Charnley et al. ([2001]).
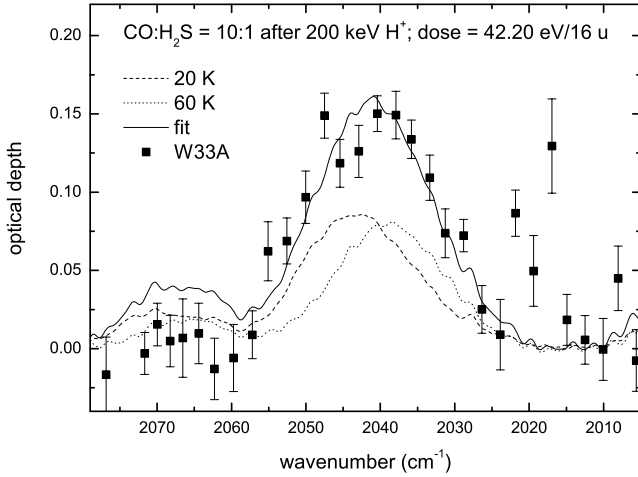

Fig. 8. Comparison between the fit obtained by the band of OCS observed in the CO:H_2S = 10:1 mixture at the end of irradiation at 20 K and warmed at 60 K and the band at 4.9 μm in W33A observed with the IRTF (Palumbo et al. [1995]).

temperatures is justified because the observed OCS band likely originates in regions of different temperature, as was demonstrated previously e.g. by Ioppolo et al. ([2009]) for the observed CO_2 band. We also tried a quantitative comparison of the amount of OCS formed after irradiation in the mixture CO:H_2S = 10:1 and the amount of OCS measured in the spectra of some YSOs. In our experiment, the ratio between the abundance of OCS and the initial abundance of H_2S is, at maximum, of about 0.025 (see Fig. 6). The fractional abundance of sulfur in the gas phase in the diffuse ISM ranges between 10^{-6}–10^{-5} with respect to H, as will be discussed further in the next. If we assume that all sulfur was condensed in the ice mantles of dust grains and formed H_2S by hydrogenation, the amount of OCS that can be formed is of the order of 2.5×10^{-8}–10^{-7}, with respect to H. This ratio is comparable to the observed values in YSOs (Table 8). As said, layered ices are presently considered a better representation of the icy mantles in interstellar dust. The profile of the OCS band obtained in our CO:H_2S layered experiment is similar to that obtained from mixture 1. In Fig. 8, we show the fit with spectra from mixture 1 because they are much less noisy than those obtained from layers.

As already discussed (see point 1), in the case of CO:H_2S mixtures we observed the production of CS_2. In all of the cases the relative amount of CS_2 is higher (of the order of 4–6 times) with respect to OCS. Moreover, at the maximum doses reached in our experiments, we can clearly see that the produced amount of OCS reaches the saturation level while we still observe an increase of the CS_2 abundance. So far, CS_2 has not been observed

in the solid phase in the interstellar medium and this can be due to the fact that its main band at about 6.60 μm (1515 cm^{-1}) overlaps with the well-known 6.00 and 6.85 μm features (e.g. Keane et al. [2001]; Boogert et al. [2008]). The IR spectrum of W33A in the 6.60 μm region has an optical depth of about 1.3 (Schutte & Khanna [2003]), while the OCS band has an optical depth of about 0.15 (see Fig. 8). In our experiment on the CO:H_2S = 10:1 mixture, the maximum value of the ratio between the optical depth of CS_2 and OCS is 5. Thus in the spectrum of W33A a hypothetical band of CS_2 should have an optical depth of about 0.75 and whose observation would be inhibited.

As reported in Table 8, the observed fractional abundance of SO_2 is about an order of magnitude higher than that of OCS. Our experimental results (see Fig. 6) show that after ion irradiation, the amount of SO_2 formed with respect to initial H_2S is about an order of magnitude higher than OCS.

The irradiation of targets containing H_2S led to the formation of a sulfur rich residuum (see Sect. 3) that has no IR bands, thus being not observable. We suggest that solid sulfur and CS_2 produced by cosmic ion irradiation could contribute to the missing sulfur problem. Early low-resolution studies using the *International Ultraviolet Explorer* (IUE) gave relatively low elemental abundances of sulfur ($\sim 4 \times 10^{-6}$), with respect to H, in the diffuse ISM (van Steenbergen & Shull [1988]), while studies using the *Goddard High Resolution Spectrograph* (GHRS) on the Hubble Space Telescope revealed that most of the sulfur is in the gas phase and its abundance is 1.5×10^{-5} with respect to H (Sofia et al. [1994]). The most recent value of sulfur cosmic abundance with respect to H defined by Lodders ([2003]) is 1.8×10^{-5} calculated on the basis of solar photospheric and meteoritic chondrite abundances, consistent with the observations in the diffuse interstellar medium. However, observations and gas-grain models of dense molecular clouds indicate that the gas phase sulfur abundance is about two orders of magnitude lower. For example, in the model of molecular evolution of a star-forming core, Aikawa et al. ([2008]) used a value of S abundance of 9.14×10^{-8}. Garrod et al. ([2007]) obtained H_2S gas abundance values in line with typical observed values, assuming an initial abundance of S of 8.0×10^{-8}, in agreement with Graedel et al. ([1982]). Other chemical models with low initial sulfur abundances (2×10^{-7}, 6×10^{-9}) can be found in Millar & Herbst ([1990]) and Doty et al. ([2002]). Thus, in molecular clouds, theoretical gas-phase chemistry models require very low elemental sulfur abundances in order to explain the observations of sulfur-bearing molecules. Where is the missing sulfur? As said, we suggest that the missing sulfur is locked up in icy grain mantles as a solid residuum and/or molecules produced by cosmic ion irradiation of ices containing H_2S. This latter is rapidly destroyed to produce OCS and SO_2 (as observed) and other sulfur bearing molecules.

References

Aikawa, Y., Wakelam, V., Garrod, R. T., et al. 2008, ApJ, 674, 984
Allamandola, L. J., Sandford, S. A., Tielens, A. G. G. M., et al. 1992, ApJ, 399, 134
Baratta, G. A., & Palumbo, M. E. 1998, J. Opt. Soc. Am. A, 15, 3076
Baratta, G. A., Palumbo, M. E., & Strazzulla, G. 2000, A&A, 357, 1045
Boogert, A. C. A., Schutte, W. A., Tielens, A. G. G. M., et al. 1996, A&A, 315, L377
Boogert, A. C. A., Schutte, W. A., Helmich, F. P., Tielens, A. G. G. M., & Wooden, D. H. 1997, A&A, 317, 929
Boogert, A. C. A., Pontoppidan, K. M., Knez, C., et al. 2008, ApJ, 678, 985
Brown, W. L., Augustyniak, W. M., Macartonio, K. J., et al. 1984, Nucl. Instr. Meth. Phys. Res. B, 1, 307
Brunetto, R., Barucci, M. A., Dotto, E., et al. 2006, ApJ, 644, 646
Charnley, S. B., Ehrenfreund, P., & Kuan, Y. J. 2001, Spectrochim. Acta A, 57, 685
Doty, S. D., van Dishoeck, E. F., van der Tak, F. F. S., et al. 2002, A&A, 389, 446
Ferrante, R. F., Moore, M. H., Spiliotis, M. M., et al. 2008, ApJ, 684, 1210
Fraser, H. J., Collings, M. P., Dever, J. W., et al. 2004, MNRAS, 353, 59
Fulvio, D., Sivaraman, B., Baratta, G. A., Palumbo, M. E., & Mason, N. J. 2009, Spectrochim. Acta A, 72, 1007
Garozzo, M., Fulvio, D., Gomis, O., Palumbo, M. E., & Strazzulla, G. 2008, Planet. Space Sci., 56, 1300
Garrod, R. T., Wakelam, V., & Herbst, E. 2007, A&A, 467, 1103
Geballe, T. R., Baas, R., Greenberg, J. M., et al. 1985, A&A, 146, L6
Gibb, E. L., Whittet, D. C. B., Boogert, A. C. A., et al. 2004, ApJS, 151, 35
Gomis, O., & Strazzulla, G. 2005, Icarus, 177, 570
Gomis, O., & Strazzulla, G. 2008, Icarus, 194, 146
Graedel, T. E., Langer, W. D., & Frerking, M. A. 1982, ApJS, 48, 321
Greenberg, M. 1982, Comets, ed. L. L. Wilkening (Tucson: The University of Arizona Press), 131
Grim, R. J. A., Baas, F., Greenberg, J. M., Geballe, T. R., & Schutte, W. 1991, A&A, 243, 473
Hatchell, J., Thompson, M. A., Millar, T. J., et al. 1998, A&A, 338, 713
Hudgins, D. M., Sandford, S. A., Allamandola, L. J., et al. 1993, ApJS, 86, 713
Ioppolo, S., Palumbo, M. E., Baratta, G. A., et al. 2009, A&A, 493, 1017
Jiang, G. J., Person, W. B., & Brown, K. G. 1975, J. Chem. Phys., 62, 1201
Keane, J. V., Tielens, A. G. G. M., Boogert, A. C. A., Schutte, W. A., & Whittet, D. C. B. 2001, A&A, 376, 254
Leto, G., & Baratta, G. A. 2003, A&A, 397, 7
Lodders, K. 2003, ApJ, 591, 1220
Loeffler, M. J., Baratta, G. A., Palumbo, M. E., Strazzulla, G., & Baragiola, R. A. 2005, A&A, 435, 587
Loeffler, M. J., Raut, U., & Baragiola, R. A. 2006, ApJ, 649, L133
Mennella, V., Baratta, G. A., Esposito, A., Ferini, G., & Pendleton, Y. J. 2003, ApJ, 587, 727
Mennella, V., Palumbo, M. E., & Baratta, G. A. 2004, ApJ, 615, 1073
Millar, T. J., & Herbst, E. 1990, A&A, 231, 466
Moore, M. H. 1984, Icarus, 59, 114
Moore, M. H., Ferrante, R. F., Hudson R. L., & Stone, J. N. 2007a, Icarus, 190, 260
Moore, M. H., Hudson, R. L., & Carlson, R. W. 2007b, Icarus, 189, 409

Palumbo, M. E. 2006, A&A, 453, 903
Palumbo, M. E., Tielens, A. G. G. M., & Tokunaga, A. T. 1995, ApJ, 449, 674
Palumbo, M. E., Geballe, T. R., & Tielens, A. G. G. M. 1997, ApJ, 479, 839
Palumbo, M. E., Strazzulla, G., Pendleton, Y. J., et al. 2000, ApJ, 534, 801
Palumbo, M. E., Baratta, G. A., Collings, M. P., et al. 2006, Phys. Chem., 8, 279
Palumbo, M. E., Leto, P., Siringo, C., & et al. 2008, ApJ, 685, 1033
Pugh, L. A., & Rao, K. N. 1976, Molecular Spectroscopy: Modern research, III (New York: Academic Press)
Rudolph, R. N. 1977, Ph.D. Thesis (Boulder: University of Colorado)
Schutte, W. A., & Khanna, R. K. 2003, A&A, 398, 1049
Smith, M. A. H., Rinsland, C. P., Fridovich, B., et al. 1985, Molecular Spectroscopy: Modern research, III (New York: Academic Press)
Smith, R. G. 1991, MNRAS, 249, 172
Sofia, U. J., Cardelli, J. A., & Savage, B. D. 1994, ApJ, 430, 650
Strazzulla, G., Leto, G., Baratta, G. A., et al. 1991, J. Geophys. Res., 96, 17547
Strazzulla, G., Baratta G. A., & Palumbo M. E. 2001, Spectrochim. Acta, 57, 825
Strazzulla, G., Leto, G., Spinella, F., et al. 2005, Astrobiology, 5, 612
Strazzulla, G., Garozzo, M., & Gomis, O. 2009, AdSpR, 43, 1442
van Steenbergen, M. E., & Shull, J. M. 1988, ApJ, 330, 942
Tielens, A. G. G. M., Tokunaga, A. T., Geballe, T. R., et al. 1991, ApJ, 381, 181
Yamada, H., & Person, W. B. 1964, J. Chem. Phys., 41, 2478
Zasowski, G., Kemper, F., Watson, D. M., et al. 2009, ApJ, 694, 459
Ziegler, J. F., Biersack, J. P., & Littmark, U. 1996, The stopping and range of ions in solids. (New York: Pergamon Press, see also http://www.srim.org)

Appendix A:

Here we define the correlation between the radiation dose used in the laboratory and the timescale in the interstellar clouds. It is important to note that chemical modification of icy target observed after ion irradiation depends, to a first approximation, on the amount of energy that ions release into the target (dose in eV molecule^{-1}) and not on the type of ion. Dose is defined as the product of ion flux (Φ; ions cm^{-2} s^{-1}), stopping power (S; eV cm^2 molecule^{-1}) and time (t; s). The product of ions flux and time is the fluence (ions cm^{-2}). Thus the time spent by grain mantles in the dense interstellar cloud to absorb a given dose is:

$$t_{\text{ISM}} = \frac{\text{Fluence}_{\text{lab}} \times S_{\text{lab}}}{\Phi_{\text{ISM}} \times S_{\text{ISM}}} \tag{A.1}$$

where the flux Φ and stopping power S of the ions in the interstellar medium have to be estimated. In this case, the approximation of monoenergetic protons has been adopted. This approximation relies on the estimation of a proton flux, usually at 1 MeV, which gives rise to the H ionization rate produced by the cosmic-ion spectrum in the ISM. This flux, estimated by Mennella et al. (2003), is $\Phi(1\text{ MeV})_{\text{ISM}} = 1$ cm^{-2} s^{-1} = 3.16×10^7 cm^{-2} years^{-1}. The stopping power of 1 MeV protons calculated by using the SRIM software (Ziegler et al. 1996) considering the targets used in our experiments is about 2.7 times that of the 200 keV protons that we used in the laboratory.